IJIE

The International Journal of Integrated Engineering

Optimization of Vortex Tube Design and Performance for Cooling Milling Process

Agus Sifa[1*], Tito Endramawan[1], M. Iksan Safi'i[1], Wardika[2]

[1]Department of Mechanical Engineering,
 Politeknik Negeri Indramayu Jl.Lohebener No.8 Lohbener- Indramayu, 45151, INDONESIA

[2]Department of Refrigeration and Air Conditioning,
 Politeknik Negeri Indramayu Jl.Lohebener No.8 Lohbener- Indramayu, 45151, INDONESIA

*Corresponding Author

Abstract: The manufacturing process is required to improve cleanliness and reduce environmental pollution and the exploration of natural resources is limited. One of the manufacturing processes is machining, especially the milling process. The phenomenon during the milling process friction occurs when the workpiece is cut by the milling tool, the effect friction between tool and workpiece occurs temperature rise. To reduce the temperature, rise of the milling tool during the workpiece cutting process, an effective and efficient alternative cooling is needed through the use of vortex tubes. The research method was carried out using the Computational Fluid Dynamic (CFD) approach and experiments with the use of inlet pressure = 1-5 Bar, and the parameters of variations in valve shape, number of nozzles, and pipe lengths. The overall results of the CFD and experiment of parameters in inlet pressure on the number of nozzles, valve shapes, and tube lengths, have an impact on the increasing inlet pressure, the higher the thermodynamic characteristics that occur in the vortex tube, but there is a loss of outlet pressure in each parameter. The geometry of the vortex tube selected is the number of nozzles 6, valve fillet shape, and tube length of 50 mm, vortex tube can be used for cooling the milling tool with the addition of a flexible hose at 5 cm from the tooltip.

Keywords: Vortex tube, milling tool, cooling, optimization, performance

1. Introduction

The current manufacturing process demands an increase in cleanliness and does not cause environmental pollution from manufacturing process waste, as well as limiting the very high exploration of natural resources. The impact of the manufacturing process is also required to reduce emissions, environmental, social [1], and health impacts [2]. One of the manufacturing processes is the machining process [3]. The machining process, especially the milling process, is required to be more environmentally friendly. The process of slicing the material with the milling process is influenced by several parameters. In the milling process, the existing parameters are tool geometry [3], cutting depth, cutting speed, cutting force, tool treatment, tool coating, and type of tool and workpiece material [4]. During the workpiece cutting process, friction occurs between the workpiece area and the tool, causing high heat [5]. The heat that occurs in the workpiece and tool due to the milling process is a major problem. At this time, to reduce the coolant cost in the milling process, the dry milling method is used [5]. The dry milling method has an impact on high cutting temperatures at high speeds [6]. The use of a vortex tube (VT) can reduce the temperature in the milling process [7].

VT is a cooling device with a mechanical system that can separate high-pressure gas streams into low-pressure hot and cold streams [8]. The distribution of temperature, pressure, and velocity components is obtained to understand the flow characteristics in VT [8]. Analysis of VT geometry on performance with different parameters, pressure inlet pin,

control valve [9], cold mass fraction ratio, and the number of nozzles [10] to be more effective and efficient. Different VT geometry as a parameter to determine the optimization of VT performance [11].

Masoud Bovand et al. have conducted a VT optimization study as a low-cost alternative refrigerant, stating that straight VT tubes are better than curved VT tubes. Several parameters to improve the phenomenon of thermal separation and diffusion process on VT on diameter, length, number, and size of nozzles [12]. Rutika Godbole and P.A. Ramakrishna have evaluated the VT design stating that the RR correlation factor as well as inlet conditions of pressure, temperature, and inlet area can be achieved [13]. Hamdan M.O et al. has investigated the VT performance, which is influenced by several main parameters, namely the inlet pressure pin, tube length tube diameter, and tube tapering angle, where the greater the inlet temperature, the greater the cold temperature difference, and the length of the tube affects the performance of the vortex tube [14]. Attala et al. have conducted experiments and stated that the characteristic thermodynamic equation correlates with cold mass fraction, cold temperature difference, and the number of nozzles [15]. Kandil and Abdelghany have conducted a Computational Fluid Dynamic investigation stating that apart from the geometry of the main component parameters that affect VT performance, the addition of fins and the effect of the orifice diameter ratio can reduce the cold outlet temperature [16]. Yunpeng Xue et al. stated to predict the VT performance with variable geometry parameters, both experimental and numerical methods [17]. Graciela S. V. et al. have recommended cooling in the machining-turning process by combining MQL-VT [18]. Luka C. et al. have improved cooling using VT in the hard milling process to efficiently reduce tool wear, roughness, and tool capability compared to the dry milling process [19]. Pradeep K. G. et al. optimizes the VT cooling position which can reduce friction, temperature and increase tool life [20].

Based on the above problems, to reduce the use of fluid coolant in the milling process to reduce the heat loss that occurs due to tool and workpiece friction, an alternative cooling with innovations is the application of VT in the milling process, where the purpose of this study is to find suitable VT characteristics for milling. In the milling process that produces the lowest cold temperature, it is necessary to optimize the design and performance of VT from the parameters of the variation of the valve shape, the number of nozzles, and the length of the tube in the VT, where the VT product can be used as an alternative solution for cooling the milling process.

2. Method

2.1 CFD 3D Model

The VT design is made into a 3D model, in this study a Computational Fluid Dynamic (CFD) approach was used using a 3D model [21], as shown in Fig. 1. Based on Table 1, obtained from the experimental results of air from the compressor engine, with power capacity of 7.5 Kw, maximum pressure of 9.75 Bar, and maximum inlet temperature of 46 °C, the CFD process used several input parameters [22]. The main parameter is the variation of inlet pressure between 1-5 Bars [23]. Pressure variations are carried out to determine the thermodynamic characteristics that occur in the VT [24]. Fig. 1 3D model using Flow Simulation for CFD of VT, CFD aims to determine the flow rate characteristics of temperature, velocity, and pressure [21]. Cold temperature difference data is used to determine the cold mass fraction ratio, Thermal Power, and Coefficient of Power (CoP), the VT design has a length of 116 mm and a cold exit diameter of 28 mm. Some of the main components that determine VT performance are varied to get the best CoP. Variations of components used are the number of nozzles, valve shape, and tube length.

Table1 - Parameters input CFD

Pressure Inlet- P_{in} (Bar)	Temperature-$T_{in.}$ (^{0}C)	Velocity-V_{in} (m/s)
1	28	11
2	28	14
3	28	17
4	28	20
5	28	23

2.2 Experiments

The VT product is made according to a 3D model design and used on a milling machine to determine the effect on the tool in milling, and the input parameters refer to in Table 1, the experimental set-up is present in Fig. 2. Experimental data in the form of velocity, temperature, and pressure. The instrument used during the experiment was to collect pressure data using a pressure gauge, collect temperature data using a thermal image camera and thermostat (Thermocouple Type-K) [23], and collect air velocity data using a digital anemometer with input parameters in Table 1.
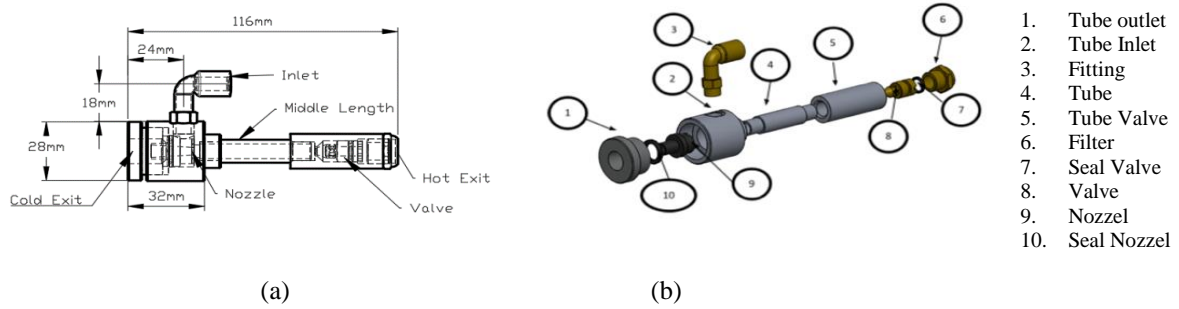
	1. Tube outlet
	2. Tube Inlet
	3. Fitting
	4. Tube
	5. Tube Valve
	6. Filter
	7. Seal Valve
	8. Valve
	9. Nozzel
	10. Seal Nozzle

(a)   (b)

Fig.1 - 3D Model design and VT and Dimensions (a) dimension of VT, and; (b) components of VT

(a)   (b)   (c)   (d)
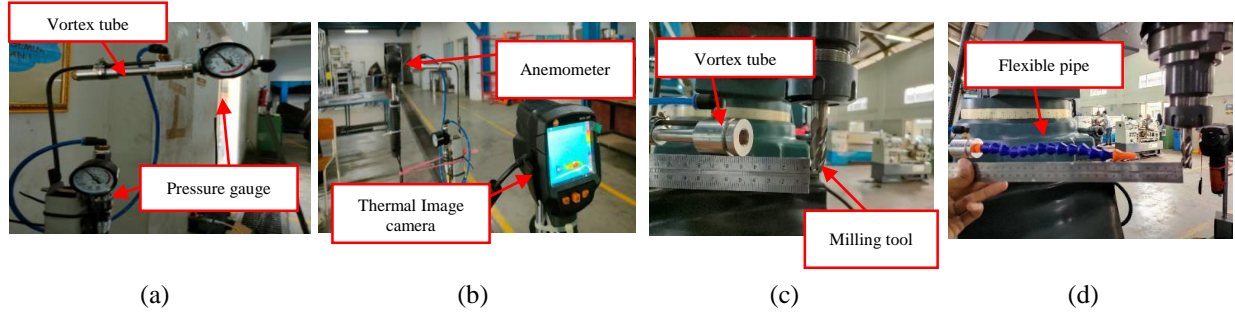
Fig. 2 - Experimental design (a) measure pressure; (b) measure velocity and temperature; (c) distance Vortex Tube on milling tool

3. Governing Equations of Thermodynamic

Ratio Cold Mass Fraction, Cold Temperature Difference, Thermal Power and Coffecient of Performance are determined as bellow, respectively:

$$\xi = \frac{\dot{m}_c}{\dot{m}_{in}} \qquad (1)$$

Where: ξ = mass fraction ratio, $\dot{m}_c$= cold mass fraction (Kg/s), $\dot{m}_{in}$= mass fraction inlet (Kg/s) [25].

$$\Delta T_c = T_{in} - T_c \qquad (2)$$

Where: T_{in} = temperature inlet (ᵒC), T_c = cold air temperature (ᵒC) [26].

$$\dot{Q}_c = \dot{m}_c c_p (T_i - T_c) \qquad (3)$$

Where: $\dot{Q}_c$= thermal power (Watt), $\dot{m}_c$= cold mass fraction (Kg/s), T_{in}= temperature inlet, T_c= cold temperature, C_p= specific heat of air (J/Kg.C)[26].

$$RE = m.\, C_p.\, \Delta T \qquad (4)$$

Where: RE = refrigeration effect, m = mass flow rate (Kg/s), Cp = specific heat of air (Kj/Kg.s), ΔT = temperature of cooling air (ᵒC), The equation used to determine work done is explained in the equation [27].

$$Work\ Done = \frac{3600}{E} x \frac{2}{t} x 10^3 \qquad (5)$$

Where: E = compressor energy (Kg/s), t = time (S), after obtaining the value of the required equations, the equation in finding the coefficient of performance (CoP) value is [27]:

$$COP = \frac{Refrigeration}{Work\ Done} \qquad (6)$$

4. Results and Discussion

4.1 Nozzle

VT optimization is carried out with a variety of nozzles, with the number of nozzles 4, 6, and 8 as shown in Fig. 3. Variations in the number of nozzles are carried out with CFD and experiments, with valve length = 60 mm, and the valve

used is a cone type. The nozzle has a diameter, $\emptyset$= 14.5 mm and a length, L = 18.5 mm, the material used is Polylactic Acid (PLA). In the CFD with variations in the number of nozzles as shown in Fig. 4 where it is showed the results of the CFD 3D model visually with the parameters of the pressure, velocity and temperature, and pressure inlet, P_{in} = 5 Bar with a variation of the number of nozzles 8, where a point is taken at a certain node to be compared with the experimental results.
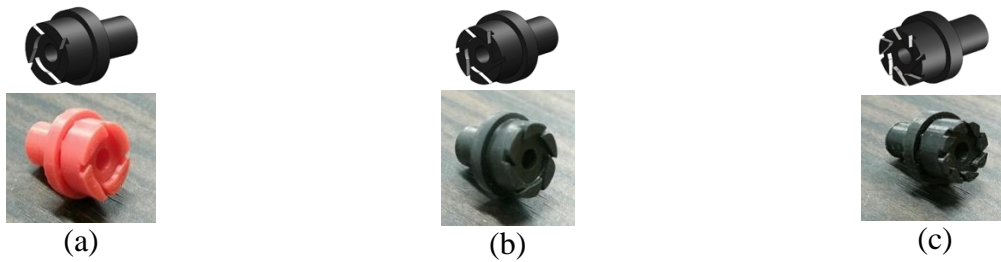

(a)   (b)   (c)

Fig. 3 - Variation number of nozzles (a) 4 nozzles; (b) 6 nozzles, and; (c) 8 nozzles
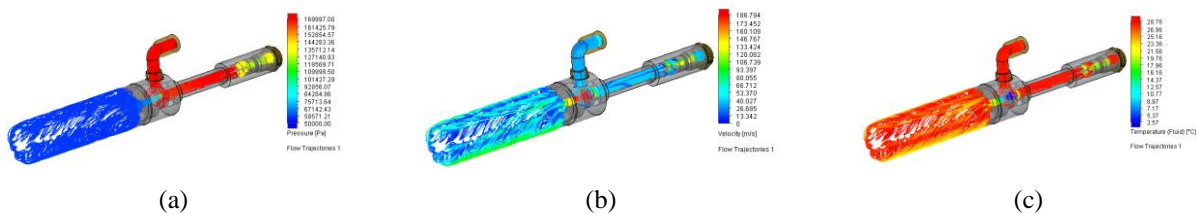

(a)   (b)   (c)

Fig. 4 - Results of CFD 3D model – nozzel (a) pressure; (b) velocity, and; (c) temperature

Table 2 - CFD results in variations in the number of nozzles

Pressure Inlet (Bar)	CFD								
	Nozzel-4 (Cold Outlet)			Nozzel-6 (Cold Outlet)			Nozzel-8 (Cold Outlet)		
	Pressure (Bar)	Velocity (m/s)	Temperature (ºC)	Pressure (Bar)	Velocity (m/s)	Temperature (ºC)	Pressure (Bar)	Velocity (m/s)	Temperature (ºC)
1	0.5	14.978	26.9	0.7	10.385	27.89	0.6	12.705	27.78
2	1.3	16.373	26.55	0.9	11.753	26.3	1.2	14.451	27.17
3	1.5	18.261	26.33	0.9	16.269	24.07	1.4	17.604	26.88
4	1.7	19.844	25.62	0.9	18.266	23.52	1.7	18.542	25.24
5	1.9	**24.409**	25.16	1.2	19.46	**23.4**	3.4	21.308	25.14

Table 2 and Table 3 Overall, the results of CFD and experiments on nozzle variations experienced a decrease in temperature at the cold exit [28]. Table 2 presents the results of the CFD simulation with variations in the number of nozzles, data on pressure, speed, and temperature at the cold outlet VT is presented. The CFD results from the variation in the number of nozzles can be seen that the highest value of cold air velocity (V_c) is at the number of nozzles 4, V_c = 24.409 m/s at the inlet pressure of 5 Bar, while the lowest cold temperature (T_c) value is owned by nozzle 6 of 23. 4 ºC. Table 3 shows the results of experiments with variations in the number of nozzles, and obtained data on pressure, velocity, and temperature at the cold outlet VT. The experimental results show that the highest cold air velocity is owned by the nozzle with an amount of 6, V_c = 13.3 m/s at the inlet pressure of 5 Bar, while the minimum temperature at the nozzle with an amount of 6, T_c = 24 ºC. From CFD data and experiments with pressure variations, it shows that there is a pressure effect, the greater the inlet pressure P_in, the greater the velocity of cold air that occurs, and the higher the inlet pressure, the lower the cold temperature obtained [29], but at the outlet, VT cold outlet pressure loss occurs.

Table 3 - Results of experiments with variations in the number of nozzles

Pressure Inlet (Bar)	Experiments								
	Nozzel-4 (Cold Outlet)			Nozzel-6 (Cold Outlet)			Nozzel-8 (Cold Outlet)		
	Pressure (Bar)	Velocity (m/s)	Temperature (ºC)	Pressure (Bar)	Velocity (m/s)	Temperature (ºC)	Pressure (Bar)	Velocity (m/s)	Temperature (ºC)
1	0,5	4,96	30,1	0,1	2,23	28,2	0,6	1,88	30,3
2	1,15	7,82	28	0,3	3,26	26,2	1,4	3,81	29,3
3	1,6	9,76	27,3	0,5	3,74	25,1	2,1	5,42	28,6
4	2,2	11,5	27,1	0,9	4,88	24,7	2,75	6,9	28,6
5	3	**13,3**	26,9	1,2	5,3	**24**	3,25	6,86	28

The thermodynamic characteristics of CFD and experimental results on variations in the number of nozzles 4, 6, and 8 can be shown in Fig. 5, all graphs show the same trend [28], the inlet pressure parameter dominantly affects the thermodynamic characteristic of VT [28]. Fig. 5(a) shows the value of the cold mass fraction ratio, and the results of the CFD simulation and experiment, in Fig. 5(a) shows the highest value, P_{in} = 5 bar, and the experimental results with the number 6 nozzle variation shown on the purple line have a ratio of values the highest cold mass fraction, ξ = 1.027, the higher the inlet pressure P_{in} impact the higher the cold mass fraction ratio [30]. Fig. 5(b) shows the CoP value of the nozzle variation from the CFD and Experiment results, the highest CoP is owned by the number 6 nozzle variation in the experiment, CoP = 0.36. Fig. 5(c) shows the cold temperature difference, the results of CFD and the experimental highest value are shown in the purple line with nozzle number 6, ΔT_c = 8ºC. The higher the cold temperature difference and the higher the cold mass fraction ratio, has graph show the same trend, and the best choice of the nozzle variation is present at the inlet pressure, P_{in} = 5 Bar with the number of nozzles 6 [31].

The thermal power value present in Fig. 5(d), the purple line shows a maximum thermal power of 35.17 Watt, in the experimental results with nozzle number 6. Based on the variations of the pressure inlet, the CoP of VT on the nozzle variation shows the higher the pressure inlet, the higher the thermodynamic characteristic [30], and the result of the calculation of the thermodynamic characteristic, which has the maximum value in the experimental results with the number of nozzles 6 [23], the nozzle shape affects the pressure outlet [32], but the number of nozzles 8 has value is lower thermodynamic characteristic than the number of nozzles six and being the best choice, this does not indicate the influence of the number of nozzles[33].
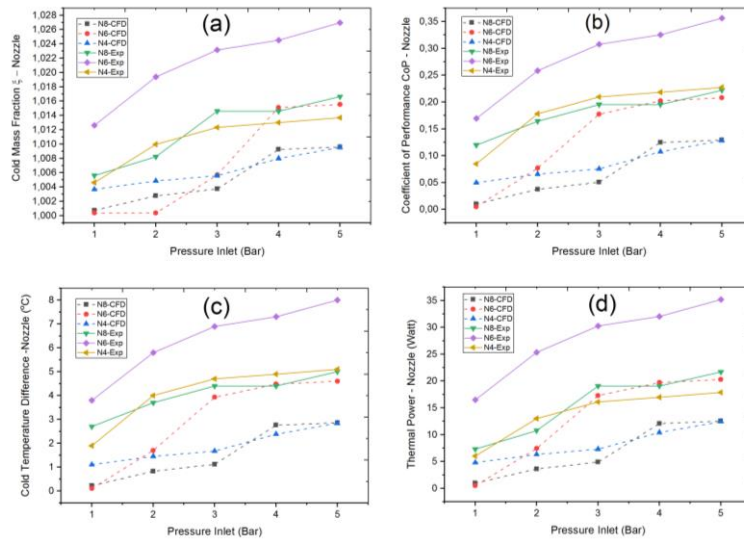

Fig. 5 - Characteristic of Vortex Tube (nozzle) (a) cold mass fraction-nozzle; (b) CoP-nozzle; (c) cold temperature difference-nozzle, and; (d) thermal power-nozzle

4.2 Valve

Variation of valve shape for optimization of VT design and performance with three types of valve shapes, namely cone, dome, and fillet, as shown in Fig. 6, the material used is brass, Fig. 6(a) is a valve cone shape [28]. Fig. 6(b) valve dome shape, and Fig. 6(c) valve fillet shape. The results of CFD are present in Fig. 7, which shows the values of pressure, velocity, and temperature. The results of CFD for variations in valve shape with pressure inlet, P_{in} between 1-5 Bar, where a point is taken at a node to compare with the results experiment. Table 4 is the result of CFD from valve variations, where the CFD results show an increase in velocity along with an increase in inlet pressure, this occurs at the fillet valve, V_c = 18.896 m/s, and the velocity profile shows the blowing force at VT [34]. The lowest temperature occurs on the valve fillet, T_c = 16.7 C. Table 4 shows the overall results of CFD, the greater the inlet pressure, the smaller the cold outlet temperature that occurs. Table 5 presenting the results experiment of VT with variations in the valve shape, the experimental results show that the highest velocity of cold air out is in the valve fillet, V_c = 4.2 m/s at a pressure of 5 Bar, and the lowest cold temperature outlet, T_c =17.5 ºC. The results of CFD and experiments VT with valve shape variations are present in Fig. 8. The calculation results of the cold mass fraction ratio are present in Fig. 8(a), CoP in Fig. 8(b), and the calculation results of cold temperature difference are present in Fig. 8 (c), while Fig. 8(d) shows thermal power.

Table 4 - CFD results with valve variations

Pressure Inlet (Bar)	CFD								
	Cone (Cold Outlet)			Dome (Cold Outlet)			Fillet (Cold Outlet)		
	Pressure (Bar)	Velocity (m/s)	Temperature (ºC)	Pressure (Bar)	Velocity (m/s)	Temperature (ºC)	Pressure (Bar)	Velocity (m/s)	Temperature (ºC)

1	0.5	10.142	27.61	0.6	10.848	27.31	0.59	9.289	25.57
2	0.8	13.583	26.77	0.9	12.984	26.25	0.61	13.551	22.38
3	1.06	14.235	25.56	1.4	14.936	25.91	0.66	14.768	20.28
4	1.6	16.087	23.87	1.9	16.476	23.78	0.87	17.159	18.79
5	1.9	18.221	21.95	2	18.524	21.31	0.98	**18.896**	**16.7**

(a)   (b)   (c)

Fig. 6 - Shape of valve (a) cone; (b) dome, and; (c) fillet
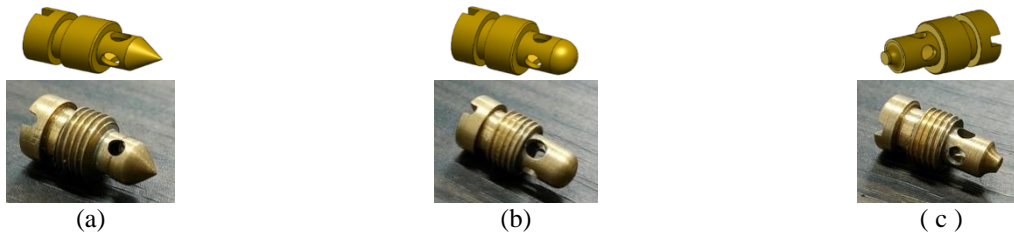

(a)   (b)   (c)
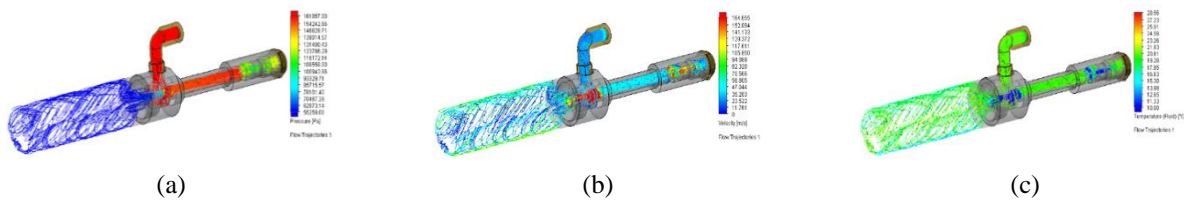
Fig. 7 - Results of CFD 3-D model (valve) (a) pressure; (b) velocity, and; (c) temperature

Table 5 - Results of experiments with variations of valve

| Pressure Inlet (Bar)	Experiments								
	Cone (Cold Outlet)			Dome (Cold Outlet)			Fillet (Cold Outlet)		
	Pressure (Bar)	Velocity (m/s)	Temperature (ºC)	Pressure (Bar)	Velocity (m/s)	Temperature (ºC)	Pressure (Bar)	Velocity (m/s)	Temperature (ºC)
1	0.25	1.68	26.1	0.08	2.13	26.1	0.05	1.5	25.5
2	0.7	2.27	24.9	1.25	2	24.9	0.08	2.6	22.7
3	1.25	3.08	23.7	1.5	2.75	23.7	0.15	3.2	20.6
4	1.75	3.27	21.8	1.75	3.31	21.8	0.25	3.5	19.4
5	2.1	3.68	21.4	2	3.53	21.4	0.75	**4.2**	**17.5**
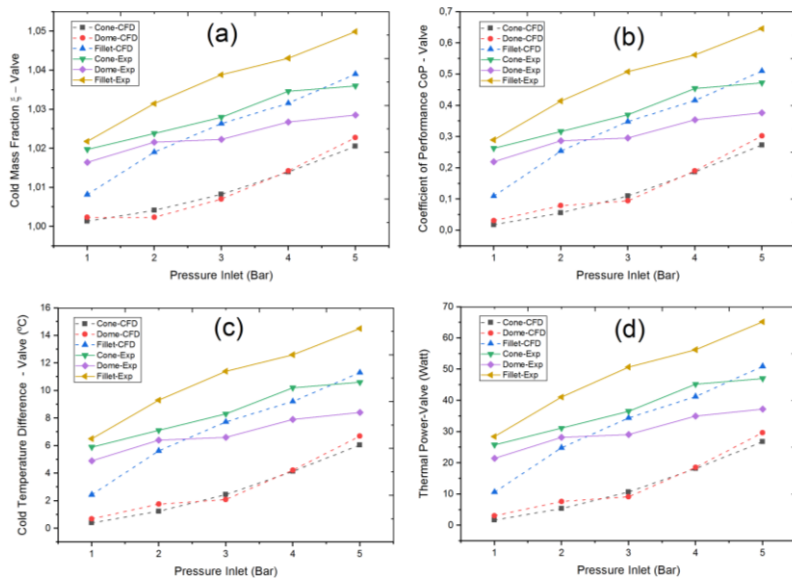
Fig. 8 - Characteristics of thermodynamic VT (Valve) (a) cold mass fraction-valve; (b) CoP-valve; (c) cold temperature difference-valve, and; (d) thermal power-valve

Fig. 8 presents the VT characteristic based on variations in valve shape. Fig. 8(a) shows the results of CFD and experiments from Cold Mass Fraction. The highest cold mass fraction ratio is the fillet valve at a pressure of 5 Bar [23],

ξ= 1.05. Fig. 8(b) presents the CoP value of CFD and experimental results. The highest CoP value is owned by the valve fillet shape in the experimental results with a pressure of 5 Bar, CoP = 0.65. Overall, the valve shape affects the VT performance [23].

Cold Temperature Difference in the results of CFD and experiments with variations in valve shape is shown in Fig. 8(c). The highest value is indicated by the yellow line owned by the valve fillet, and the highest value of cold temperature difference, ΔT_c = 14.5 ºC, where the cold temperature difference can affect the cold mass fraction ratio [29]. Fig. 8(d) presents the CFD and experimental results from the value of the thermal power. The graph from the experiments and CFD results present a high value in a valve fillet, and the best choice of thermal power at the experimental results has a pressure of 5 Bar with the thermal power of 65 Watt. The results of the CFD and experiments based on variations in valve shape shows that there is an influence of pressure. The greater the inlet pressure of the given, the greater the characteristic of thermodynamics on the VT, where an increase in cold temperature difference will affect the increase in thermal power [25] and on variations in valve shape. VT has the best thermodynamic characteristics in the form of a valve fillet.

4.3 Length

The VT in this study was variations with a length of 30 mm, 40 mm, and 50 mm, where the material used was Aluminum. The variations in tube length can present in Fig. 9. Fig. 10 is the result of CFD from VT with variations in tube length with a Pin inlet pressure of 5 Bar and a tube length of 50 mm. Fig. 10(a) is a picture of the trajectory pressure that occurs in the VT, Fig. 10(b) visually shows the trajectory velocity, and Fig. 10(c) is the trajectory temperature of VT.
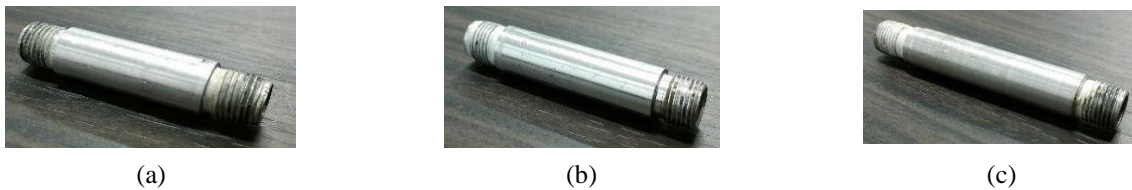

| (a) | (b) | (c) |

Fig. 9 - Tube Length variation; (a) 30mm; (b) 40mm, and; (c) 50mm
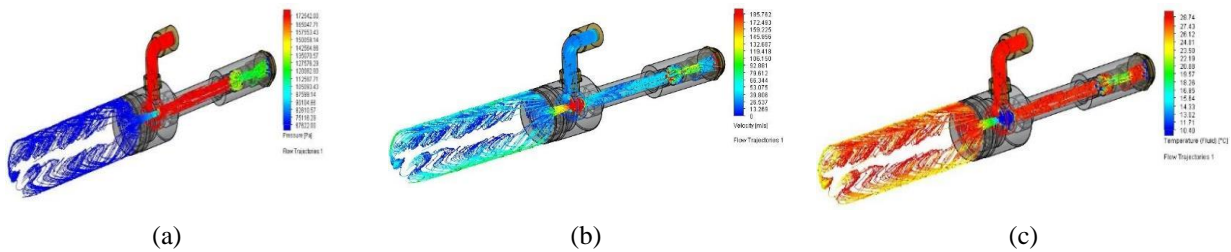

| (a) | (b) | (c) |

Fig. 10 - Results of CFD 3-D model (length) (a) pressure; (b) velocity, and; (c) temperature

Table 6 - CFD results in variations in length

Pressure Inlet (Bar)	CFD								
	Length 30 mm (Cold Outlet)			Length 40 mm (Cold Outlet)			Length 50 mm (Cold Outlet)		
	Pressure (Bar)	Velocity (m/s)	Temperature (ºC)	Pressure (Bar)	Velocity (m/s)	Temperature (ºC)	Pressure (Bar)	Velocity (m/s)	Temperature (ºC)
1	0.69	11.461	27.49	0.75	10.385	27.89	0.58	10.777	26.82
2	0.88	12.336	26.73	0.87	11.753	26.3	0.95	11.416	26.26
3	1.38	14.232	25.45	0.89	16.269	24.07	1.30	13.529	24.11
4	1.51	17.791	25.26	0.90	18.266	23.52	1.52	17.594	23.89
5	1.87	**20.547**	23.75	1.21	19.46	23.4	1.82	20.067	**22.98**

Table 6. present CFD results of VT with variations in length, where the VT have a long tube of 30 mm highest velocity, while the lowest cold temperature is owned by a 50 mm long tube at a pressure of 5 Bar. The inlet pressure affects the cold pressure outlet, cold outlet velocity, and cold outlet temperature. The greater the inlet pressure Pin, the greater the cold outlet air velocity that occurs at VT, and the lower the cold temperature [35], but there is a temperature loss in each tube length. Table 7 shows the experimental data with the VT having the highest velocity outlet velocity at length tube 40 mm, and VT highest cold temperature at length tube 50 mm length, T_c = 23.6 ºC with a pressure of 5 Bar. The results of CFD and experiments are present at the outlet pressure of the VT occurs a pressure loss and the data results from variations in inlet pressure. Table 7 present that the greater the inlet pressure in the length variation, the higher the thermodynamic characteristics of the VT [36]. Tube length of VT has an essential role in reducing cold temperature [37].

Table 7 - Experimental results with variations in length

Pressure Inlet (Bar)	Experiments								
	Length 30 mm (Cold Outlet)			Length 40 mm (Cold Outlet)			Length 50 mm (Cold Outlet)		
	Pressure (Bar)	Velocity (m/s)	Temperature (ºC)	Pressure (Bar)	Velocity (m/s)	Temperature (ºC)	Pressure (Bar)	Velocity (m/s)	Temperature (ºC)
1	0.2	1	27.9	0.1	2.23	28.2	0.3	1.43	28
2	0.8	1.58	27.5	0.3	3.26	26.2	0.8	2.13	25.1
3	1.25	1.98	27	0.5	3.74	25.1	1.25	2.65	24.4
4	1.6	2.81	27	0.9	4.88	24.7	1.65	2.7	23.9
5	2.2	3.11	26.9	1.2	**5.3**	24	2	3.64	**23.6**

The calculation results of thermodynamic characteristics from various lengths are present in Fig.11. The cold mass fraction ratio calculation is indicated in Fig. 11(a), CoP is present in Fig. 11(b), the cold temperature difference calculation is presented in Fig. 11(c), and thermal power calculation is shown in Fig. 11(d). The results of CFD and experiments shown in Fig. 11 are based on variations in pressure inlet affecting the outlet temperature [38]. Fig. 11 shows the value of cold mass fraction from CFD and experiments results, the experimental results have a higher value of cold mass fraction than the CFD results, the highest value of cold mass fraction at a pressure of 5 Bar is shown on the yellow line, ξ = 1.017. The longer the VT tube, it will affect the VT performance [38], and the long tube and the mass fraction ratio influence each other, when the air inlet flows through the tube wall friction occurs, this has an impact on the cold mass fraction ratio and cold temperature difference [38]. There is a relationship between the ratio of cold mass fraction and the cold temperature difference [21]. Overall, geometric variations in the form of variations in the number of nozzles, valve shapes, and tube lengths affect the thermodynamic characteristic of VT [39]. The higher the inlet pressure applied to the tube length, the lows the cold outlet temperature [24]. The highest tube length has a high value of cold mass fraction [40] and affects thermal power that occurs, cold mass fraction affects the cold temperature difference [41][42]. Overall the pressure inlet affects the thermodynamic characteristics of VT.
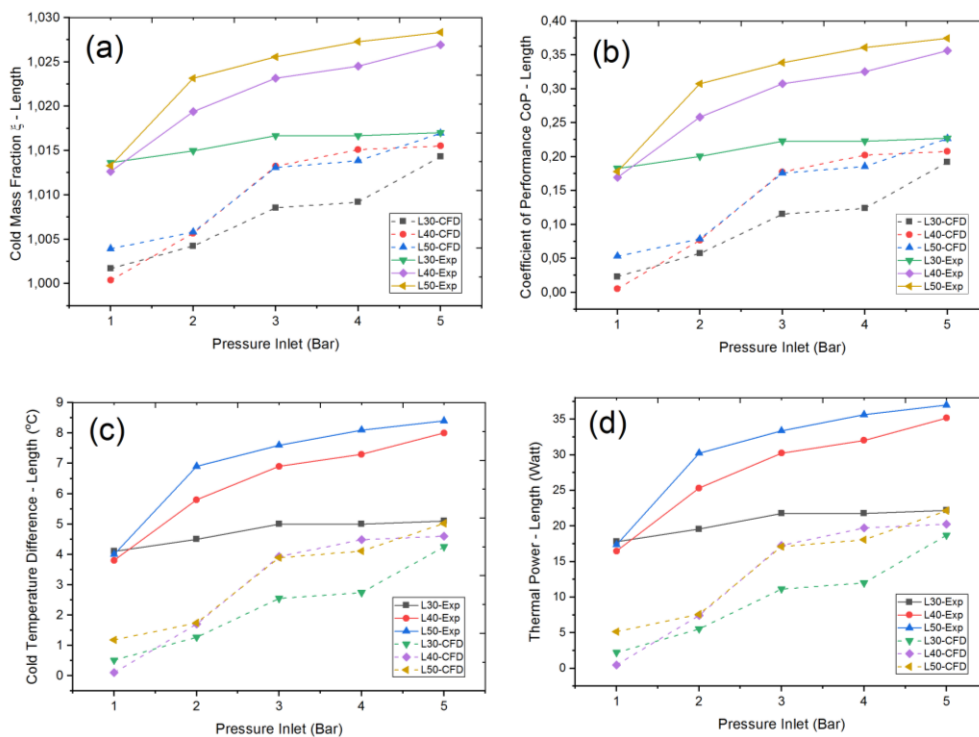

Fig. 11 - Characteristics of Vortex Tube-length(a) cold mass fraction-length; (b) CoP-length; (c) cold temperature difference-length, and; (d) thermal power-length

4.4 Tool Milling Temperature

Cooling experiments were also carried out on the milling tool, using an inlet pressure of 1-5 Bar, varying the distance of 5 cm, 10 cm, and 15 cm between the VT and the milling tool, to determine the maximum temperature on milling tool is affected the cooling VT. When cooling experiment using the cooling VT, then the convection cooling process occurs [36]. Additional use of flexible hose must see the effects. The temperature was measured on the milling tool using cooling the VT with a thermostat. The measuring temperature results compare the test results using a flexible hose and without a flexible hose. The experiment results without and using a flexible hose with length tube variation are present in Table 8.

Table 8 - Temperature difference cooling tool milling test based on distance on tube length variation

Distance (cm)	Use hose Temperature (C)			Without hose Temperature (C)		
	L30mm	L40mm	L50mm	L30mm	L40mm	L50mm
5	1.8	3.8	5.6	1.4	3.2	3.8
10	1	3	2.4	0.8	1.4	1.8
15	0.4	1.6	1.2	0.4	1	1.4

Table 8 shows the results of temperature measurements on a milling tool using a VT cooler with variations in tube length. Add a flexible hose to the vortex tube for optimization of VT performance. Parameter measurement performed by VT on the milling tool uses the distance from the end of the flexible hose to the milling tool. The measurement distance is between 5 cm, 10 cm, and 15 cm, as well as variations in tube lengths of 30 mm, 40 mm, and 50 mm. The measurement temperature results show that the cooling distance affects the temperature in the milling tool. The highest temperature on the milling tool occurred at a long tube of 50 mm, with the addition of a flexible hose having a temperature difference of 5.6 °C and without a flexible hose of 3.8 °C. The results of temperature measurements on the milling tool show that the use of flexible hoses can increase the temperature drop in the milling tool so that the use of flexible hoses on vortex tubes with a tube length of 50 mm is better than without flexible hoses. Table 9 shows the temperature measurement on the milling tool using cooling of VT with valve variations. The measurement temperature results show that the maximum temperature difference value occurs at 5 cm, with a valve fillet form with used a flexible hose, $\Delta T = 9.8$ °C, and without using a flexible hose of 7.8 °C, the use of a fillet valve, the temperature value obtained is lower than without a flexible hose.

Table 9 - Temperature difference cooling test of milling tool based on distance on valve variation

Distance (cm)	Use hose Temperature (C)			Without hose Temperature (C)		
	Cone	Dome	Fillet	Cone	Dome	Fillet
5	8.2	7	9.8	7.5	6.8	7.8
10	3.4	3.8	4.6	3.2	3.8	3.6
15	2.4	2	2.2	2.2	1.8	1.4

Table 10 - Temperature difference cooling tool milling test based on distance in nozzle variation

Distance (cm)	Use hose Temperature (°C)			Without hose Temperature (°C)		
	N4	N6	N8	N4	N6	N8
5	3.6	4.4	2.2	1.6	3.2	1.6
10	1.8	3	1.2	0.8	1.4	0.6
15	1.6	1.6	0.6	0.6	1	0.4

Based on the data in Table 10, the experimental results show the effect of VT cooling with distances variations to the milling tool, the best choice temperature difference was obtained on the variation of the vortex tube component with 5 cm, the number of nozzles 6 had the highest temperature difference value. The use of a flexible hose, $\Delta T = 4.4$ °C and without the use of a flexible hose, $\Delta T = 3.2$ °C, so that the use of nozzle variations has a higher value at 5 cm and a nozzle with a total of 6. Overall, from the optimization of the shaped valve, the number of nozzles, and the tube lengths, the higher the given air pressure inlet will have an impact on the lower the temperature at the cold outlet [36]. Design optimization with the CFD approach is more effective and experiments are used to validate the results of CFD, where the optimization design that has been carried out shows a correlation between the number of nozzles, tube length, and valve shape on the VT performance [43]. VT geometry is the main parameter in determining the VT criteria [44]. This shows that it is effective in reducing the temperature and can be applied to cool the milling process [35].

5. Conclusion

In this research to optimize the design and performance of vortex tubes with variations in pressure inlet, with variations in the number of nozzles, valve shapes, and tube lengths, from the CFD and experiments results can be concluded that:

1. The results of the CFD and the experiment, overall, the variations in inlet pressure on the number of nozzles, valve shapes, and tube lengths have an impact on increasing the thermodynamic characteristics of vortex tube, but that is a loss of pressure at the outlet for each parameter.

2. In the variation in the number of nozzles that have the lowest cold temperature and the highest vortex tube characteristic, the nozzle variation is number nozzle 6.

3. Variations in valve shape, with approach CFD and experimentally, show the lowest cold temperature results and the highest thermodynamic characteristics have occurred in the valve fillet form.

4. The length tube variations have the lowest cold temperature, and the highest thermodynamic characteristic is owned a tube length of 50 mm.

5. The results of the cooling test on the milling tool, nearest the distance of the milling tool are the best choice, and the use of flexible hoses can increase the cold temperature.

Acknowledgement

References

[1] Goindi, G. S., & Sarkar, P. (2017). Dry machining: a step towards sustainable machining– challenges and future directions. *Journal of cleaner production*, *165*, 1557-1571.

[2] Ismail, N. I. K., Sani, A. S. A., & Rosli, N. (2021). Study of oil flow rates effects on lubricant oil behaviour during minimum quantity lubrication milling process. *Materials Today: Proceedings*, *46*, 1635-1639.

[3] Bhirud, N. L., & Gawande, R. R. (2017). Measurement and prediction of cutting temperatures during dry milling: review and discussions. *Journal of the Brazilian Society of Mechanical Sciences and Engineering*, *39*(12), 5135-5158.

[4] Tahmasebi, E., Albertelli, P., Lucchini, T., Monno, M., & Mussi, V. (2019). CFD and experimental analysis of the coolant flow in cryogenic milling. *International Journal of Machine Tools and Manufacture*, *140*, 20-33.

[5] Le Coz, G., Marinescu, M., Devillez, A., Dudzinski, D., & Velnom, L. (2012). Measuring temperature of rotating cutting tools: Application to MQL drilling and dry milling of aerospace alloys. *Applied Thermal Engineering*, *36*, 434-441.

[6] Deshpande, S., & Deshpande, Y. (2019). A review on cooling systems used in machining processes. *Materials Today: Proceedings*, *18*, 5019-5031.

[7] Saravanan, P., Raj, D. S., Hussain, S., Shankar, V. R., & Raj, N. (2021). Optimization of jet position and investigation of the effects of multijet MQCL during end milling of Ti-6Al-4V. *Journal of Manufacturing Processes*, *64*, 392-408.

[8] Pouraria, H., & Park, W. G. (2014). Numerical investigation on cooling performance of Ranque-Hilsch vortex tube. Thermal Science, 18(4), 1173-1189.

[9] Acar, M. S., Erbas, O., & Arslan, O. (2019). The performance of vapor compression cooling system aided Ranque-Hilsch vortex tube. Thermal Science, 23(2 Part B), 1189-1201.

[10] Rafiee, S., & Sadeghiazad, M. (2016). Experimental and 3D-CFD study on optimization of control valve diameter for a convergent vortex tube. Frontiers in Heat and Mass Transfer (FHMT), 7(1).

[11] Chiappini, D., Mendecka, B., & Bella, G. (2021). Sizing and Optimization of a Vortex Tube for Electric Vehicle HVAC Purposes. SAE Technical Paper, 24-0099.

[12] Bovand, M., Valipour, M. S., Eiamsa-Ard, S., & Tamayol, A. (2014). Numerical analysis for curved vortex tube optimization. *International Communications in Heat and Mass Transfer*, *50*, 98-107.

[13] Godbole, R., & Ramakrishna, P. A. (2020). Design guidelines for the vortex tube. *Experimental Thermal and Fluid Science*, *118*, 110169.

[14] Hamdan, M. O., Al-Omari, S. A., & Oweimer, A. S. (2018). Experimental study of vortex tube energy separation under different tube design. *Experimental Thermal and Fluid Science*, *91*, 306-311.

[15] Attalla, M., Ahmed, H., Ahmed, M. S., & El-Wafa, A. A. (2017). An experimental study of nozzle number on Ranque Hilsch counter-flow vortex tube. *Experimental Thermal and Fluid Science*, *82*, 381-389.

[16] Kandil, H. A., & Abdelghany, S. T. (2015). Computational investigation of different effects on the performance of the Ranque–Hilsch vortex tube. *Energy*, *84*, 207-218.

[17] Xue, Y., Arjomandi, M., & Kelso, R. (2013). The working principle of a vortex tube. *international journal of refrigeration*, *36*(6), 1730-1740.

[18] Šterpin Valić, G., Kostadin, T., Cukor, G., & Fabić, M. (2023). Sustainable Machining: MQL Technique Combined with the Vortex Tube Cooling When Turning Martensitic Stainless Steel X20Cr13. Machines, 11(3), 336.

[19] Celent, L., Bajić, D., Jozić, S., & Mladineo, M. (2023). Hard Milling Process Based on Compressed Cold Air-Cooling Using Vortex Tube for Sustainable and Smart Manufacturing. Machines, 11(2), 264.

[20] Saravanan, P., Raj, D. S., Hussain, S., Shankar, V. R., & Raj, N. (2021). Optimization of jet position and investigation of the effects of multijet MQCL during end milling of Ti-6Al-4V. Journal of Manufacturing Processes, 64, 392-408.

[21] Alsaghir, A. M., Hamdan, M. O., & Orhan, M. F. (2021). Evaluating velocity and temperature fields for Ranque–Hilsch vortex tube using numerical simulation. International Journal of Thermofluids, 10, 100074.

[22] Pouraria, H., & Zangooee, M. R. (2012). Numerical investigation of vortex tube refrigerator with a divergent hot tube. Energy Procedia, 14, 1554-1559.

[23] Cartlidge, J., Chowdhury, N., & Povey, T. (2022). Performance characteristics of a divergent vortex tube. International Journal of Heat and Mass Transfer, 186, 122497.

[24] Pourmahmoud, N., Zadeh, H. A., Moutaby, O., & Bramo, A. (2014). Numerical investigation of operating pressure effects on the performance of a vortex tube. *Thermal Science*, *18*(2), 507-520.

[25] Bazgir, A. (2017). Investigation of the effects of number of nozzle intakes on the performance of vortex tube refrigerators base on CFD. In 6th International Conference on Research in Engineering and Technology, London, June (Vol. 2, pp. 16-29).

[26] Pourmahmoud, N., Abbaszadeh, M., & Rashidzadeh, M. (2016). Numerical simulation of effect of shell heat transfer on the vortex tube performance. International Journal of Heat and Technology, 34(2), 293-301.

[27] Karthik, S. (2015). Design and Computation of COP of Vortex Tube. *International Journal of Scientific and Engineering Research*.

[28] Im, S. Y., & Yu, S. S. (2012). Effects of geometric parameters on the separated air flow temperature of a vortex tube for design optimization. *Energy*, *37*(1), 154-160.

[29] Rafiee, S. E., & Rahimi, M. (2013). Experimental study and three-dimensional (3D) computational fluid dynamics CFD) analysis on the effect of the convergence ratio, pressure inlet and number of nozzle intake on vortex tube performance–Validation and CFD optimization. *Energy*, *63*, 195-204.

[30] Manickam, M., & Prabakaran, J. (2022). Effect of number of the nozzle and cold mass fraction on the performance of counter flow vortex tube using the computational fluid dynamic analysis. International Journal of Ambient Energy, 43(1), 1134-1146.

[31] Alsaghir, A. M., Hamdan, M. O., Orhan, M. F., & Awad, M. (2022). Numerical and Sensitivity Analyses of Various Design Parameters to Maximize Performance of a Vortex Tube. International Journal of Thermofluids, 100133.

[32] Sankar Ram, T., & Anish Raj, K. (2013). An experimental performance study of vortex tube refrigeration system. International Journal Of Engineering Development And Research.

[33] Pourmahmoud, N., Esmaily, R., & Hassanzadeh, A. (2015). CFD investigation of vortex tube length effect as a designing criterion. International Journal of Heat and Technology, 33(1), 129-136.

[34] Xue, Y., Binns, J. R., Arjomandi, M., & Yan, H. (2019). Experimental investigation of the flow characteristics within a vortex tube with different configurations. *International Journal of Heat and Fluid Flow*, *75*, 195-208.

[35] Thakare, H. R., & Parekh, A. D. (2020). Experimental investigation of Ranque—Hilsch vortex tube and techno– Economical evaluation of its industrial utility. *Applied Thermal Engineering*, *169*, 114934.

[36] Agrawal, N., Naik, S. S., & Gawale, Y. P. (2014). Experimental investigation of vortex tube using natural substances. *International communications in heat and mass transfer*, *52*, 51-55.

[37] Rafiee, S. E., & Sadeghiazad, M. M. (2017). Experimental and 3D CFD analysis on optimization of geometrical parameters of parallel vortex tube cyclone separator. *Aerospace science and technology*, *63*, 110-122.

[38] Alsaghir, A. M., Hamdan, M. O., Orhan, M. F., & Awad, M. (2022). Numerical and Sensitivity Analyses of Various Design Parameters to Maximize Performance of a Vortex Tube. International Journal of Thermofluids, 100133.

[39] Khazaei, H., Teymourtash, A. R., & Malek-Jafarian, M. (2012). Effects of gas properties and geometrical parameters on performance of a vortex tube. Scientia Iranica, 19(3), 454-462.

[40] Moraveji, A., & Toghraie, D. (2017). Computational fluid dynamics simulation of heat transfers and fluid flow characteristics in a vortex tube by considering the various parameters. *International Journal of Heat and Mass Transfer*, *113*, 432-443.

[41] Rafiee, S. E., & Sadeghiazad, M. M. (2016). Heat and mass transfer between cold and hot vortex cores inside Ranque-Hilsch vortex tube-optimization of hot tube length. International Journal of Heat and Technology, 34(1), 31-38.

[42] Bramo, R. A., & Pourmahmoud, N. (2011). CFD simulation of length to diameter ratio effects on the energy separation in a vortex tube. Thermal Science, 15(3), 833-848.

[43] Behera, U., Paul, P. J., Kasthurirengan, S., Karunanithi, R., Ram, S. N., Dinesh, K., & Jacob, S. (2005). CFD analysis and experimental investigations towards optimizing the parameters of Ranque–Hilsch vortex tube. *International Journal of Heat and Mass Transfer*, *48*(10), 1961-1973.

[44] Sankar Ram, T., & Anish Raj, K. (2013). An experimental performance study of vortex tube refrigeration system. *International Journal of Engineering Development and Research*, vol. 1(2), 1822.